

Broad-Specificity Immunoassay for *O,O*-Diethyl Organophosphorus Pesticides: Application of Molecular Modeling to Improve Assay Sensitivity and Study Antibody Recognition

Zhen-Lin Xu,[†] Yu-Dong Shen,[†] Wen-Xu Zheng,[†] Ross C. Beier,[‡] Gui-Mian Xie,[†] Jie-Xian Dong,[†] Jin-Yi Yang,[†] Hong Wang,[†] Hong-Tao Lei,[†] Zhi-Gang She,[§] and Yuan-Ming Sun^{*,†}

Key Laboratory of Food Quality and Safety of Guangdong Province, South China Agricultural University, Guangzhou 510642, China, Food and Feed Safety Research Unit, Southern Plains Agricultural Research Center, Agricultural Research Service, U.S. Department of Agriculture, 2881 F&B Road, College Station, Texas 77845-4988, United States, and School of Chemistry and Chemical Engineering, Sun Yat-Sen University, 135 Xingangxi Road, Guangzhou 510275, China

A monoclonal antibody (mAb) against 4-(diethoxyphosphorothioxy)benzoic acid (hapten 1) was raised and used to develop a broad-specificity competitive indirect enzyme-linked immunosorbent assay (ciELISA) for 14 *O,O*-diethyl organophosphorus pesticides (OPs). Computer-assisted molecular modeling was used to model two-dimensional (2D) and three-dimensional (3D) quantitative structure–activity relationships (QSARs) to study antibody recognition. On the basis of insights obtained from the QSAR models, two heterologous coating haptens, 4-(diethoxyphosphorothioylamino)butanoic acid (hapten 2) and 4-(diethoxyphosphorothioxy)-2-methylbenzoic acid (hapten 3) were designed, synthesized, and used to develop heterologous ciELISAs with significantly improved sensitivity. The heterologous ciELISA using hapten 2 as the coating hapten showed good sensitivity in a broad-specific manner for eight *O,O*-diethyl OPs and may be used as a screening method for the determination of these OPs. Our studies demonstrated that molecular modeling can provide insights into the spatial and electronic effects of molecular structures that are important for antibody activity, which can then be used to improve immunoassay sensitivity.

Organophosphorus pesticides (OPs), a group of cholinesterase-inhibiting insecticides, have been widely used both in residential and agricultural environments because of their broad-spectrum insecticidal activity and effectiveness.¹ However, the extensive use of OPs has led to numerous poisonings of nontarget species, including human fatalities.^{1,2} It was reported that OPs are responsible for about two-thirds of the deaths from acute poisoning

in developing countries, a total of 200 000 deaths per year.³ To help prevent further OP poisonings, the addition of OP residue determination in environment samples and agricultural products is urgently needed. Although, instrumental methods such as GC/GC–MS or LC/LC–MS offer high sensitivity and specificity and have the potential for simultaneous determination of multiple analogues, the associated high-costs and time-consuming labor requirements have inhibited broadening the scope of monitoring, particularly in field-screening scenarios. As an alternative, affinity-based immunoassay techniques, such as an enzyme-linked immunosorbent assay (ELISA), fulfill the need for developing inexpensive, reliable, and effective field monitoring methods for low molecular-weight toxic molecules and have been used in many applications in environmental and agricultural monitoring.^{4,5} Immunoassays are high-throughput screening methods, and broad-specificity immunoassays are favored that are capable of simultaneously determining a class of closely related analytes because they can identify more than one target and detect positive samples from hundreds of negative samples in one simple test.⁶

Several broad-specificity immunoassays for OPs have been reported.^{7–14} These assays can detect at least four or more OPs in one test and were applied to analyze actual samples. Liang et

* To whom correspondence should be addressed. Phone: +8620-8528-3925. Fax: +8620-8528-0270. E-mail: ymsun@scau.edu.cn.

[†] South China Agricultural University.

[‡] U.S. Department of Agriculture.

[§] Sun Yat-San University.

(1) Lu, C.; Barr, D. B.; Pearson, M. A.; Waller, L. A. *Environ. Health Perspect.* **2008**, *116*, 537–542.

(2) Valdez, S. B.; Garcia, D. E. I.; Wiener, M. S. *Rev. Environ. Health.* **2000**, *15*, 399–412.

(3) Eddleston, M.; Buckley, N. A.; Eyer, P.; Dawson, A. H. *Lancet* **2008**, *371*, 597–607.

(4) Blasco, C.; Torres, C. M.; Picó, Y. *Trends Anal. Chem.* **2007**, *26*, 895–913.

(5) Suri, C. R.; Boro, R.; Nangia, Y.; Gandhi, S.; Sharma, P.; Wangoo, N.; Rajesh, K.; Shekhawat, G. S. *Trends Anal. Chem.* **2009**, *28*, 29–39.

(6) Spinks, C. A. *Trends Food Sci. Technol.* **2000**, *11*, 210–217.

(7) Sudi, J.; Heeschen, W. *Kiel. Milchwirtsch. Forschungsber.* **1988**, *40*, 179–203.

(8) Johnson, J. C.; Van Emon, J. M.; Pullman, D. R.; Keeper, K. R. *J. Agric. Food Chem.* **1998**, *46*, 3116–3123.

(9) Banks, J. N.; Chaudhry, M. Q.; Matthews, W. A.; Haverly, M.; Watkins, T.; North Way, B. *J. Food Agric. Immunol.* **1998**, *10*, 349–361.

(10) Alcocer, M. J. C.; Dillon, P. P.; Manning, B. M.; Doyen, C.; Lee, H. A.; Daly, S. J.; O'Kennedy, R.; Morgan, M. R. A. *J. Agric. Food Chem.* **2000**, *48*, 2228–2233.

(11) Jang, M. S.; Lee, S. J.; Xue, X.; Kwon, H.-M.; Ra, C. S.; Lee, Y. T.; Chung, T. *Bull. Korean Chem. Soc.* **2002**, *23*, 1116–1120.

(12) Liang, Y.; Liu, X. J.; Liu, Y.; Yu, X. Y.; Fan, M. T. *Anal. Chim. Acta* **2008**, *615*, 174–183.

(13) Liu, Y.; Lou, Y.; Xu, D.; Qian, G.; Zhang, Q.; Wu, R.; Hu, B.; Liu, F. *Microchem. J.* **2009**, *93*, 36–42.

al.¹² developed a broad-specificity ELISA for *O,O*-dimethyl OPs, and the recoveries of the assay ranged between 77.1% and 104.7% for Chinese cabbage samples spiked with malathion, dimethoate, phenthoate, phosmet, and methidathion. Piao et al.¹⁴ developed a broad-specificity ELISA with average IC₅₀ values for 12 *O,O*-diethyl phosphorothioate and phosphorodithioate OPs of 89 ng/mL, and the recoveries for several spiked food samples were from 57 ± 4.1 to 138 ± 1.9%. The good specificity and reliability of the assays indicated that the broad-specificity assays are an attractive approach to use for a rough screening of positive samples from hundreds of negative samples.

However, the development of immunoassays today is still primarily based on trial and error, especially for designing the immunizing and coating haptens. The reason for this may well exist in the lack of understanding the interactions between antibodies and antigens or haptens. From the 1990s, immunochemists have tried to utilize computer-assisted molecular modeling to help develop immunoassays for small molecules and suggested that molecular modeling is useful because it can provide insights into molecular structure and biological-activity that are difficult or otherwise impossible to obtain.¹⁵ Most of the studies used molecular modeling to help explain cross-reactivity (CR) of antibodies and structure–activity relationships (SARs). Some immunochemists tried to utilize molecular modeling to help design rational haptens. They usually designed several haptens as candidates and then used molecular modeling to optimize the energy and calculate the valences and charges. The hapten which was both structurally and electronically most similar to the target analyte was selected as the immunizing hapten. With the help of molecular modeling, several sensitive and specific immunoassays have been developed for the determination of 4,4'-dinitrocarbanilide,¹⁶ irgarol 1051,¹⁷ 2,4,6-trichloroanisole,¹⁸ permethrin,¹⁹ nonylphenyl,²⁰ and semicarbazide.²¹ However, the use of molecular modeling to study the quantitative structure–activity relationships (QSARs) of antibody recognition and improvement of the assay properties based on molecular modeling results was seldom reported. Wang et al.²² applied molecular modeling to construct a three-dimensional QSAR (3D-QSAR) model to help define the epitopes of fluoroquinolone (FQ) antibiotics recognized by an anti-FQ monoclonal antibody. They suggested a hapten to produce broad-specificity antibodies but did not demonstrate its use.

Our laboratory has had a long-term interest in developing immunochemical methods for determination of small molecules using computer-assisted molecular modeling as a tool to help

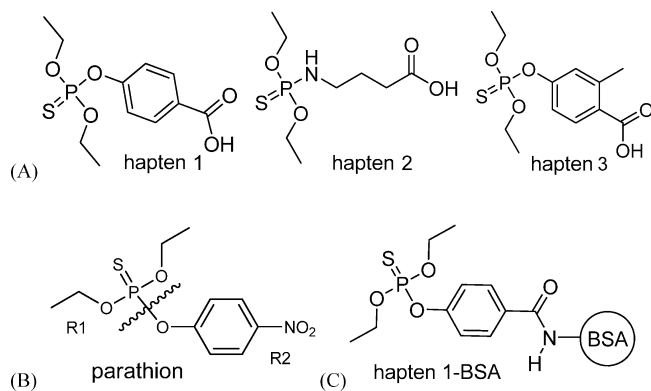


Figure 1. (A) The chemical structures of haptens (hapten 1, hapten 2, and hapten 3), (B) split of OPs to R1 and R2 fragments in topomer CoMFA (using parathion as an example), and (C) immunogen (hapten 1–BSA).

improve assay performance. Previously, we raised a polyclonal antibody (PAb) with broad-specificity for *O,O*-diethyl OPs and developed a two-dimensional QSAR (2D-QSAR) model to study antibody recognition.²³ In this work, monoclonal antibodies (MAbs) were further raised. An improved theoretical calculation method was used to optimize the structural conformations of the OPs, and multiple linear regression analysis was used to construct a 2D-QSAR model. Topomer comparative molecular field analysis (CoMFA) was also used to construct a 3D-QSAR model for further study of antibody recognition. On the basis of insights obtained from the QSAR models, two heterologous haptens (Figure 1A) were designed as new competitors, and studies described here employ these new haptens to improve assay sensitivity.

MATERIALS AND METHODS

Materials and Chemicals. *O,O*-diethyl OP standards were obtained from Dr. Ehrenstorfer GmbH (Augsburg, Germany). 4-Aminophenol was obtained from Sinopharm Chemical Reagent Co., Ltd. (Shenyang, China). 4-Hydroxy-2-methylbenzoic acid, the culture media RPMI-1640, hypoxanthine-aminopterin-thymidine (HAT), hypoxanthine-thymidine (HT), pristane, and polyethylene glycol (PEG) 2000 were obtained from Sigma-Aldrich (St. Louis, MO). Other materials and chemicals, instrumentation, buffers, and solutions were previously described.²³

Synthesis and Characterization of Haptens. *Hapten 1.* Hapten 1 was synthesized and characterized as previously described.¹⁷

Hapten 2. *O,O*-Diethyl phosphorochloridithioate (1.81 g, 9.6 mmol) was added dropwise to a stirred mixture of 4-aminobutanoic acid (0.660 g, 6.4 mmol), KOH (0.898 g, 16 mmol), and methanol (50 mL). After stirring for 12 h at 0 °C, the mixture was filtered and the solvent was removed under reduced pressure. The residue was washed several times with chloroform and filtered, and the chloroform filtrate was concentrated under reduced pressure. The residue was subjected to column chromatography (silica gel, CHCl₃–MeOH (6:1)) to give 0.91 g of hapten 2 in 56% yield. ESI-MS analysis (negative) *m/z* 254 [M – H][–]. ¹H NMR (400 MHz, CDCl₃ and TMS): δ 1.29 (t, *J* = 7.0 Hz, 6H, –CH₃); 1.79 (p, *J* = 6.9 Hz, 2H, –CH₂–); 2.41 (t, *J* = 7.3 Hz, 2H, –CH₂–);

(23) Xu, Z.-L.; Xie, G.-M.; Li, Y.-X.; Wang, B.-F.; Beier, R. C.; Lei, H.-T.; Wang, H.; Shen, Y.-D.; Sun, Y.-M. *Anal. Chim. Acta* **2009**, *647*, 90–96.

- (14) Piao, Y. Z.; Kim, Y. J.; Kim, Y. A.; Lee, H.-S.; Hammock, B. D.; Lee, Y. T. *J. Agric. Food Chem.* **2009**, *57*, 10004–10013.
 (15) Xu, Z.-L.; Shen, Y.-D.; Beier, R. C.; Yang, J.-Y.; Lei, H.-T.; Wang, H.; Sun, Y.-M. *Anal. Chim. Acta* **2009**, *647*, 125–136.
 (16) Beier, R. C.; Stanker, L. H. *Anal. Chim. Acta* **2001**, *444*, 61–67.
 (17) Ballesteros, B.; Barceló, D.; Sanchez-Baeza, F.; Camps, F.; Marco, M.-P. *Anal. Chem.* **1998**, *70*, 4004–4014.
 (18) Sanvicens, N.; Sánchez-Baeza, F.; Marco, M.-P. *J. Agric. Food Chem.* **2003**, *51*, 3924–3931.
 (19) Ahn, K. C.; Watanabe, T.; Gee, S. J.; Hammock, B. D. *J. Agric. Food Chem.* **2004**, *52*, 4583–4594.
 (20) Estévez, M.-C.; Kreuzer, M.; Sánchez-Baeza, F.; Marco, M.-P. *Environ. Sci. Technol.* **2006**, *40*, 559–568.
 (21) Vass, M.; Diblíková, I.; Cernoch, I.; Franek, M. *Anal. Chim. Acta* **2008**, *608*, 86–94.
 (22) Wang, Z.; Zhu, Y.; Ding, S.; He, F.; Beier, R. C.; Li, J.; Jiang, H.; Feng, C.; Wan, Y.; Zhang, S.; Kai, Z.; Yang, X.; Shen, J. *Anal. Chem.* **2007**, *79*, 4471–4483.

3.00 (td, $J = 6.8, 11.1$ Hz, 2H, CH₂); 3.97–4.08 (m, 4H, –CH₂–). ¹³C NMR (150 MHz, CDCl₃ and TMS): δ 15.8 (d), 26.2 (d), 30.9, 40.8 (d), 62.8 (d), 178.9. ³¹P NMR (242 MHz, CDCl₃ and TMS) δ : 71.63.

Hapten 3. *O,O*-Diethyl phosphorochloridothioate (2.26 g, 12 mmol) was added dropwise to a stirred mixture of 4-hydroxy-2-methylbenzoic acid (1.52 g, 10.0 mmol), KOH (1.40 g, 25 mmol), and methanol (50 mL). After stirring for 12 h at 0 °C, the mixture was filtered and the solvent was removed under reduced pressure. Distilled water (20 mL) was added, and the solution was extracted several times with chloroform. The water solution was acidified with 6 mol/L HCl and extracted several times with chloroform. The chloroform solution was then concentrated under reduced pressure and subjected to column chromatography (silica gel, CHCl₃–MeOH (6:1)) to give 0.84 g of hapten 3 in 27.6% yield. ESI-MS analysis (negative) m/z 303 [M – H][–]. ¹H NMR (600 MHz, CDCl₃ and TMS): δ 1.38 (t, $J = 7.09$ Hz, 6H, –CH₃); 2.66 (s, 3H, CH₃), 4.26 (qd, $J = 14.21, 7.08$ Hz, 4H, –CH₂), 7.09 (s, 1H, ArH), 7.11 (d, $J = 8.92$ Hz, 1H, ArH), 8.09 (d, $J = 8.58$ Hz, 1H, ArH). ¹³C NMR (150 MHz, CDCl₃ and TMS): δ 15.9 (d), 22.3, 65.3 (d), 118.2 (d), 124.0 (d), 125.0, 133.3, 144.0, 154.0 (d), 171.9. ³¹P NMR (242 MHz, CDCl₃ and TMS): δ 62.16.

Preparation and Characterization of Hapten–Protein Conjugates. Hapten–protein conjugates were synthesized by the active ester method.²⁴ Hapten 1 was coupled to carrier protein bovine serum albumin (BSA) for immunogen (hapten 1-BSA), and all the haptens were coupled to ovalbumin (OVA) for coating antigens (hapten 1–OVA, hapten 2–OVA, and hapten 3–OVA). Details of the synthesis method and characterization of the obtained conjugates were similar to those previously described.²³

Production of mAbs. Immunization. BALB/c female mice aged 6–8 weeks (supplied by the Guangdong Medical Laboratory Animal Center) were immunized subcutaneously with a 1:1 (v/v, 200 μ L) mixture of an immunogen (100 μ g) in PBS and Freund's complete adjuvant. Booster injections were given intraperitoneally with the same amount of immunogen emulsified with incomplete Freund's adjuvant at 3 week intervals after the initial injection. After 1 week from each booster injection, mice were tail-bled and the antisera were tested for antihapten antibody titer by indirect ELISA using a homologous coating antigen. After a resting period of 3 weeks following the third injection, one mouse that exhibited the best titer for each immunogen was selected as the donor of spleen cells for hybridoma production. Each selected mouse received a final intraperitoneal injection with the same amount of immunogen in PBS, and 3 days following the final injection the mice were sacrificed for cell fusion.

Cell Fusion, Hybridoma Selection, and Cloning. The hybridoma cells were acquired by fusion of the spleen cells isolated from the selected mice with SP2/0 murine myeloma cells using PEG 2000 by the same procedure as described by Kane and Banks.²⁵ At 8 to 10 days after cell fusion, when the hybridoma cells were grown to approximately 30–40% confluent in the well, culture supernatants were collected and screened using indirect ELISA for the presence of antihapten antibodies. Selected hybridomas were cloned by limiting dilution, and stable antibody-producing

clones were expanded. A competitive indirect ELISA (ciELISA), the protocol of which was described below, was then employed to determine if the antibodies could recognize the analytes. Selected clones were used for antibody production by ascites growth. Ascites fluids were collected and purified using a protein-G column and were used in the following ELISA.

Optimized ciELISA Protocol. The ciELISA protocol used was similar to that previously reported.¹⁷ Briefly, polystyrene 96-well microtiter plates were coated (100 μ L/well) with hapten 1–OVA (20 ng/mL), hapten 2–OVA (30 ng/mL), or hapten 3–OVA (50 ng/mL) and incubated at 4 °C overnight, the plates were washed 5 times with PBST (PBS containing 0.05% Tween-20) solution and blocked with skim milk (200 μ L/well) for 2 h, and then washed 2 times with PBST solution. OP standards were dissolved in PBS containing 5% methanol and applied to the plate at 50 μ L/well. The mAb was diluted with PBST solution (1:96 000, 1:64 000, and 1:64 000 for the above coating antigens, respectively) and was added at 50 μ L/well, incubated for 40 min, and then washed 5 times with PBST solution. IgG-HRP diluted 1:6 000 in PBST was added (100 μ L/well). After incubation for 40 min, the plate was washed 5 times with PBST solution, TMB solution was added to the wells (100 μ L/well), and the plate was incubated for 10 min. The reaction was stopped by addition of 2 M H₂SO₄ (50 μ L/well), and the absorbance was recorded at 450 nm ($A_{450\text{nm}}$). Competitive curves were obtained by plotting the normalized signal (B/B_0) against the logarithm of analyte concentration. The 50% inhibition value (IC_{50}) and limit of detection (IC_{10} , LOD) were obtained from a four-parameter logistic equation of the sigmoidal curve²⁶ using OriginPro 7.5 software (OriginLab Corporation, Northampton, MA).

Cross-Reactivity Determination. The cross-reactivity (CR) values were calculated according to the following equation:

$$(IC_{50}(\text{hapten, mol/L})/IC_{50}(\text{cross-reactant, mol/L})) \times 100 \quad (1)$$

Molecular Modeling. 2D-QSAR. The ground state geometries of all molecules were optimized at the Becke3LYP level of density functional theory (DFT-B3LYP)^{27,28} with the Gaussian 03 package (revision B.05, Gaussian, Inc., Pittsburgh, PA). The P, S, Cl, and Br atoms were described using the LANL2DZ basis set, including a double- ξ valence basis set with the Hay and Wadt effective core potential (ECP).²⁹ An additional d polarization shell was added for P, S, Cl, and Br with an exponent of 0.340, 0.421, 0.514, and 0.389, respectively.³⁰ The 6-31G(d,p) basis set was used for all other atoms. Physicochemical and topological molecular descriptors based on the optimized structures, such as the highest occupied molecular orbital energy (E_{HOMO}), the lowest unoccupied molecular orbital energy (E_{LUMO}), the energy difference between the HOMO and the LUMO ($\Delta E_{\text{H-L}}$), log of the octanol/water partition coefficient (log P), dipole moment (μ), surface area (S), molecular volume (V), molar refractivity (R),

(26) Hennon, M.-C.; Barcelo, D. *Anal. Chim. Acta* **1998**, *362*, 3–34.

(27) Becke, A. D. *J. Chem. Phys.* **1993**, *98*, 5648–5652.

(28) Lee, C.; Yang, W.; Parr, R. G. *Phys. Rev. B* **1988**, *37*, 785–789.

(29) Hay, P. J.; Wadt, W. R. *J. Chem. Phys.* **1985**, *82*, 299–310.

(30) Huzinaga, S.; Andzelm, J.; Klobukowski, M.; Radzio-Andzelm, E.; Sakai, Y.; Tatewaki, H. *Gaussian Basis Sets for Molecular Calculations*; Elsevier: Amsterdam, The Netherlands, 1984.

(24) Weetall, H. H. *Methods Enzymol.* **1976**, *44*, 134–148.

(25) Kane, M. M.; Banks, J. N. Raising Antibodies. In *Immunoassays: A Practical Approach*; Gosling, J. P., Ed.; Oxford University Press: Oxford, U.K., 2000; pp 37–50.

hydration energy (E_{hyd}), charge on the P atom (Q_{p}), charge on the S atom (Q_{s}), and molecular weight (M_{w}) were extracted from the Gaussian files or obtained by HyperChem 7.0 software (Hypercube, Inc.).

To obtain a 2D-QSAR model, the Statistical Package for Social Scientists (SPSS) 13.0 for Windows (SPSS, Chicago, IL) was used. For QSAR descriptions, the activity data ($-\log \text{IC}_{50}$ (pIC_{50}), mol/L) was used as the dependent variable, while all the molecular descriptors were the independent variables. The descriptors having the largest correlation with the pIC_{50} were selected to perform stepwise multiple linear regression analysis. The predictive ability of the equation was evaluated by a well-known method of "leave-one-out" (LOO) cross-validation in which one compound was removed from the data set and its activity was predicted using the model built from the rest of the data set.³¹ The LOO cross-validation coefficient q^2 was obtained.

3D-QSAR. The 3D-QSAR model was constructed using topomer comparative molecular field analysis (CoMFA) modeling performed on the Sybyl 8.1 program package (Tripos Inc.) running on a HP xw6600 workstation with an Intel Xeon E5430 2.66 GHz processor. The OP structures were sketched and then geometry optimized to global low energy conformations using the standard Tripos force field with an 8 Å cutoff for nonbonded interactions in conjunction with Gasteiger–Hückel charges, a 0.005 kcal/(mol Å) termination gradient, and a dielectric constant of 4. On the basis of the structures, a spreadsheet was created and filled with the activity data (pIC_{50} , mol/L). In topomer CoMFA, OPs were separated into two fragments (R1 and R2, Figure 1B). The fragments were separated in the fragmentation algorithm and applied to the topomer alignment to make a 3D invariant representation.³² Partial least-squares (PLS)³³ methodology for cyclic cross-validation with the LOO method was used in the topomer-CoMFA to produce a series of coefficients similar to the original CoMFA. The topomer CoMFA field was used as an independent variable, and the pIC_{50} activity value was used as a dependent variable.

RESULTS AND DISCUSSION

mAb Production. The haptens were too small to induce an immune response, hence the need to render them immunogenic by linking them to a large carrier protein. Bovine serum albumin (BSA) was used as the carrier protein for immunization because it is readily available, is fully soluble, and has numerous functional groups useful for cross-linking to small molecules. Meanwhile, ovalbumin (OVA) was used as a secondary carrier (used for screening clones). The coupling ratio of hapten 1–BSA, hapten 1–OVA, hapten 2–OVA, and hapten 3–OVA was 30.6, 8.9, 8.2, and 9.6, respectively. Theoretically, there are fewer sites to interact with the antibody when OVA is used as the coating antigen, thereby producing better sensitivity than using a coating antigen with a higher load of hapten.²³

Three mice were immunized with hapten 1–BSA, and the mouse that showed the highest titer of polyclonal antiserum and the best inhibition with *O,O*-diethyl OPs in a ciELISA was selected

for cell fusion. The cells in 6 positive wells among 144 wells were subjected to cloning procedures. One hybridoma (12C2) secreting MABs with high affinity to the OPs was obtained. Finally, MABs were obtained from 12C2 by ascites production and purified using a protein-G column. The MABs isotype was determined as IgG1.

ELISA Optimization. A ciELISA using hapten 1–OVA as the coating antigen was applied to investigate the specificity and sensitivity of the obtained MABs to the OPs. ELISA conditions such as the coating concentration, mAb dilution, incubation time, IgG-HRP dilution were optimized to provide a maximum absorbance in the absence of analyte (A_{max}) in the range of 1.3–1.8 and the best sensitivity (IC_{50}). The optimized ELISA conditions were shown in the experimental section. The curves obtained with 14 OPs showed a low background (with an average A_{450} lower than 0.046), indicating no nonspecific binding was found in the test.

mAb Specificity and Sensitivity. In the development of a multiple-analyte assay, the CR is evaluated to estimate the affinity of the antibody for each of the analytes.³⁴ CR is most often calculated by using units of weight, example, nanograms/well. However, as the molecular weights of the compared compounds have a greater difference, the calculated value for CR will become more incorrect and may even be reversed, depending on the molecular size difference. CR binding is a site specific, structure specific phenomenon that is a molar dependent quantity, and therefore, CR should be calculated using units of moles, example, nanomole/milliliter.¹⁵ For this purpose, the molar CR of 14 OPs was tested using the corresponding immunizing hapten (hapten 1) as the reference compound (CR = 100%). The results are shown in Table 1 and indicate that the obtained MABs show broad-specificity with 14 OPs. The CR was higher than 100% for parathion, coumaphos, dichlofenthion, and phoxim and higher than 20% for quinalphos, triazophos, phosalone, and phorate. Although the structure of parathion is similar to the hapten which was used for immunization, the highest CR of 6447.3% was observed for coumaphos. This result might be due to a conformation change of the hapten coupled to the carrier protein. The structure of the hapten coupled to the carrier protein is shown in Figure 1C. Clearly, the formation of the amide bond results in a hapten structure that is similar to coumaphos. This may be the major reason for the high CR for coumaphos. The CR for other OPs such as chlorpyrifos and diazinon were lower than 20%, which may be due to the complex substitute elements, such as Cl, Br, and alkyl on the phenyl group. As demonstrated, the substituted elements on the phenyl are important for antibody recognition.

QSAR Studies. *2D-QSAR.* In our previous studies, the *ab initio* Hartree–Fock (HF) method with a 6-31G* basis set was used to optimize the OPs to obtain the minimum energy conformations.²³ However, the *ab initio* HF method does not include the effects of instant electronic correlation, while the DFT-B3LYP method does.³⁵ It was suggested that the DFT-B3LYP method exhibits good agreement with experiment.^{36,37} Moreover, since

(31) Tetko, I. V.; Tanchuk, V. Y.; Villa, A. E. P. *J. Chem. Inf. Comput. Sci.* **2001**, *41*, 1407–1421.

(32) Cramer, R. D. *J. Med. Chem.* **2003**, *46*, 374–388.

(33) Bush, B. L.; Nachbar, R. B., Jr. *J. Comput.-Aided Mol. Des.* **1993**, *7*, 587–619.

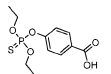
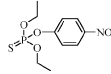
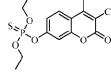
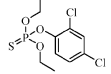
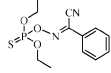
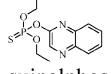
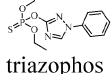
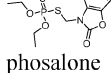
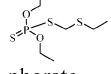
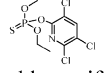
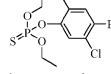
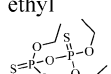
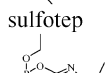
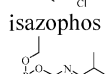
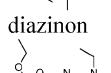
(34) Degelmann, P.; Wenger, J.; Niessner, R.; Knopp, D. *Environ. Sci. Technol.* **2004**, *38*, 6795–6802.

(35) Seminario, J. M.; Politzer, P. *Modern Density Functional Theory: A Tool for Chemistry*. In *Theoretical and Computational Chemistry*, Vol. 2; Elsevier: Amsterdam, The Netherlands, 1995.

(36) Zuilhof, H.; Dinnocenzo, J. P.; Reddy, A. C.; Shaik, S. *J. Phys. Chem.* **1996**, *100*, 15774–15784.

(37) Yan, X.-F.; Xiao, H.-M.; Gong, X.-D.; Ju, X.-H. *J. Mol. Struct. THEOCHEM* **2006**, *764*, 141–148.

Table 1. The IC₅₀ Values for O,O-Diethyl OPs in Homologous and Heterologous ciELISA^a

OPs	coating antigens								
	hapten 1-OVA			hapten 2-OVA			hapten3-OVA		
	IC ₅₀	CR	LOD	IC ₅₀	CR	LOD	IC ₅₀	CR	LOD
 hapten 1	0.4048	100.0	0.0421	0.1215	100.0	0.01347	0.1783	100.0	0.0184
 parathion	0.0215	2353.0	0.0029	0.0042	3615.3	3.5×10 ⁻⁴	0.0076	2931.9	8.9×10 ⁻⁴
 coumaphos	0.0063	6447.3	0.0007	6.02×10 ⁻⁴	20251.6	6.0×10 ⁻⁵	0.0011	16264.4	1.3×10 ⁻⁴
 dichlofenthion	0.1842	238.6	0.0144	0.0351	375.8	0.0041	0.0627	308.7	0.0064
 phoxim	0.2033	204.6	0.0194	0.0529	236.0	0.0069	0.0640	286.3	0.0074
 quinalphos	0.4225	98.5	0.0495	0.0681	183.3	0.0070	0.1002	182.9	0.0065
 triazophos	0.7104	61.5	0.1028	0.0905	144.9	0.0102	0.1362	141.3	0.0130
 phosalone	1.1348	45.2	0.1463	0.2430	63.4	0.0238	0.2816	80.2	0.0326
 phorate	1.4954	24.3	0.1855	0.4932	22.1	0.0511	0.8379	19.1	0.0803
 chlorpyrifos	4.5767	10.7	0.5778	1.2934	11.3	0.12356	2.0876	10.3	0.2287
 bromophos-ethyl	6.4081	8.6	1.2949	1.7321	9.5	0.1784	2.6732	9.1	0.3043
 sulfotep	8.6275	5.2	1.4245	2.1084	6.4	0.2162	3.5843	5.5	0.3815
 isazophos	11.6557	3.8	1.7659	4.6357	2.8	0.4591	6.9899	2.8	0.7220
 diazinon	20.5402	2.1	2.0377	6.4803	2.0	0.5850	10.8650	1.7	1.0594
 pirimiphos-ethyl	26.6127	1.8	4.3275	8.6071	1.6	0.7269	12.2669	1.7	1.2600

^a The values of IC₅₀ (μg/mL) and LOD (IC₁₀, μg/mL) were obtained from four-parameter logistic equations used to fit standard curves and were the mean of triplicate experiments.

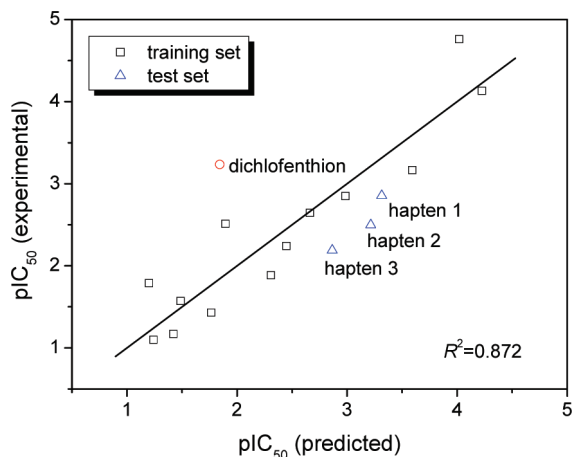


Figure 2. Plot of predicted versus experimental values (pIC_{50}) by using multiple linear regression analysis. Dichlofenthion (\circ) is considered an outlier and is not included in the plot.

the OPs contain large atoms such as P, S, Cl, and Br, the LANL2DZ basis set rather than the 6-31G basis set was suggested.³⁸ Therefore, the DFT-B3LYP method was used to optimize the OPs with basis set 6-31G* for atoms C, H, O, and N and with basis set LANL2DZ for atoms P, S, Cl, and Br.

A 2D-QSAR model was obtained based on a stepwise multiple-linear regression analysis of the OP activity data and the structural parameters. The equation of the QSAR model was as follows:

$$pIC_{50} = 4.510 - 27.430E_{LUMO} - 0.756 \log P$$

$$N = 14, R = 0.859, R^2 = 0.738, q^2 = 0.615, \quad (2)$$

$$\text{Std} = 0.6095, F = 15.453, P_F = 0.0006$$

Figure 2 presents a plot of experimental pIC_{50} values versus predicted pIC_{50} values. Dichlofenthion is an outlier in the data set due to its high residual value (1.3897). Repeating the QSAR modeling in the absence of dichlofenthion resulted in an improved correlation ($R^2 = 0.872$), compared to when dichlofenthion was included ($R^2 = 0.738$). The equation of the QSAR model can be described as follows:

$$pIC_{50} = 4.821 - 29.027 E_{LUMO} - 0.873 \log P$$

$$N = 13, R = 0.934, R^2 = 0.872, q^2 = 0.774, \quad (3)$$

$$\text{Std} = 0.4367, F = 34.132, P_F = <0.0001$$

Both the two regression models are significant ($P_F < 0.001$) using the F statistics. The models had good predictability according the cross-validated coefficient q^2 , which should be greater than 0.5 for a reliable model using the LOO method.³⁹ The QSAR model demonstrates that energy of the lowest unoccupied molecular orbital, E_{LUMO} , and log of the octanol/water partition coefficient, $\log P$, were mainly responsible for antibody recognition. These results suggest that decreasing the E_{LUMO} or $\log P$ of a compound in this chemical set might improve antibody recognition. The frontier-orbital energies and

hydrophobicity of a compound can play an important role in biological activity.⁴⁰ From the graphical representation of the parathion LUMO (Figure 3), it was apparent that the distribution of the LUMO was shown mainly with the OP phenyl substituent and not with the *O,O*-diethyl thiophosphate moiety (analogous graphical representations were also obtained for other analytes). Since all the OPs share the same *O,O*-diethyl thiophosphate moiety, the mAb sensitivity to the OPs may be influenced by this group.

3D-QSAR. CoMFA is one of the most popular methods used for quantitative structure–activity relationship (QSAR) studies at the three-dimensional (3D) level. However, there is a problem in using the standard CoMFA and that is the alignment of the series of molecular structures.³² A slight or partial shift in the alignment of molecular structures in the series can produce misleading results. The *O,O*-diethyl thiophosphate moiety was used here as the basic template for the OPs, which allowed good alignment of all compounds in the series (we tried to obtain a 3D-QSAR model using the traditional CoMFA method but failed). However, the difficulty with the CoMFA method can be overcome by using the new topomer CoMFA methodology.³² Topomer CoMFA is a comparative molecular field analysis that calculates the steric and electrostatic fields with topomerically aligned fragments. In the topomer CoMFA, every molecule is separated into two fragments which are referred to as an R series. All OPs share the same *O,O*-diethyl thiophosphate moiety, which was defined as the R1 fragment, and the substituents were defined as the R2 fragment (Figure 1B).

The topomer CoMFA analysis yielded a cross-validated correlation coefficient (q^2) of 0.565 and R^2 of 0.881 with a cross-validated standard error of the estimate of 0.41. The number of components that provide the highest q^2 are 2. These values show acceptable statistical correlation and predictability in this topomer CoMFA model.

The topomer CoMFA interaction maps (steric and electrostatic interactions) for both bromophos fragments, R1 and R2, are shown in Figure 4. No contour maps were found around the R1 fragment indicating that this commonly shared moiety did not influence antibody recognition. The contour maps around the R2 fragment showed that the structure of R2 greatly influenced antibody recognition. This is coincident with the 2D-QSAR results. The green contours indicate regions where groups with steric bulk increase activity, while yellow contours indicate regions where groups with steric bulk decrease activity. There is one green contour around the para-position of phenol (Figure 4C), which can explain the results for parathion when the para-position is substituted with a nitrile. The two yellow contours around the meta-positions suggest that increasing the groups with steric bulk will decrease the activity and may explain the low pIC_{50} of isazophos, diazinon, and pirimiphos-ethyl.

For the CoMFA electrostatic map, blue contours indicate regions where electron positive groups increase activity, and red contours indicate regions where electron negative groups increase activity. There are three blue contours around the ortho-, meta-, and para-positions, which can explain the results for dichlofenthion, quinalphos, and triazophos, in which the three positions

(38) Check, C. E.; Faust, T. O.; Bailey, J. M.; Wright, B. J.; Gilbert, T. M.; Sunderlin, L. S. *J. Phys. Chem. A* **2001**, *105*, 8111–8116.

(39) Walker, J. D.; Jaworska, J.; Comber, M. H.; Schultz, T. W.; Dearden, J. C. *Environ. Toxicol. Chem.* **2003**, *22*, 1653–65.

(40) Yao, S.-W.; Lopes, V. H. C.; Fernández, F.; García-Mera, X.; Morales, M.; Rodríguez-Borges, J. E.; Cordeiro, M. N. D. S. *Bioorg. Med. Chem.* **2003**, *11*, 4999–5006.

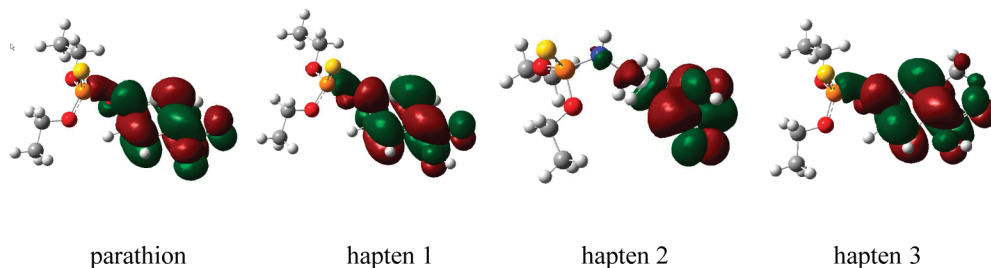


Figure 3. The graphical representation of the LUMO for parathion and haptens.

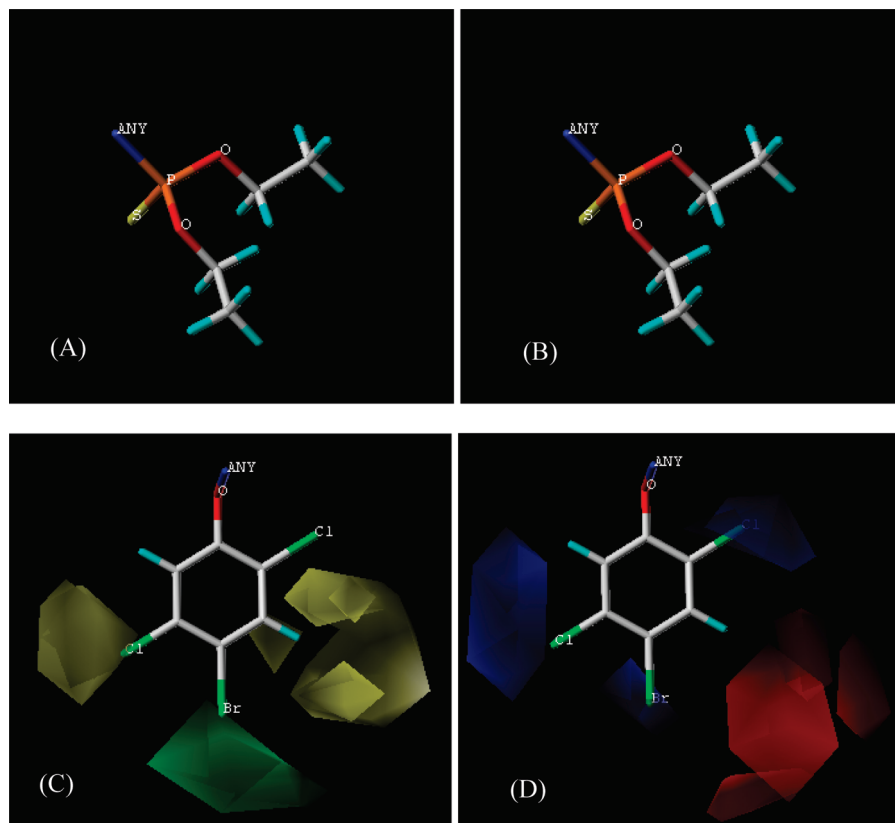


Figure 4. Topomer CoMFA contour maps represented with bromophos. Parts A and B reflect steric and electrostatic contours of fragment R1. Parts C and D reflect steric and electrostatic contours of fragment R2. For steric interactions, green is good and yellow is bad. For electrostatic interactions: blue, electron positive good, electron negative bad; red, electron positive bad, electron negative good.

are substituted with hydrogen and not with a halogen. The big red contours around the meta-position of phenol suggests that increasing the negative charge of the group at this position should increase activity. The antibody showed high-activity to coumaphos, which could be due to the carbonyl group substituted at that position. However, when the meta-position was substituted with an alkane (as in isazophos, diazinon, and pirimiphos-ethyl), antibody activity decreased significantly.

Design of Heterologous Coating Haptens. It is generally accepted that heterology between the immunizing and coating antigens is an important factor for improving sensitivity of an immunoassay.^{41,42} The use of heterologous haptens can eliminate problems associated with strong affinity of the antibodies to the spacer arm that leads to no or poor inhibition by the target compound.⁴³ However, the design of heterologous coating haptens

is generally based on trial and error. For example, a set of heterologous coating haptens were synthesized and then tested one by one.^{12,13} Also, Piao et al. performed a total of 32 ELISAs to select the most suitable coating hapten for the best ELISA results.¹⁴ It is hoped that the design of the hapten used as the coating hapten may be carried out under a more rational basis.

Assay sensitivity may be improved using a heterologous coating antigen only when a combination of antibody/coating conjugate is appropriate. Goodrow et al.⁴⁴ pointed out that for a fixed quantity of antibody, the better sensitivity was observed when the affinity of antibody for the analyte was greater than the affinity of the antibody for the coating antigen. In other words, decreasing the affinity of the antibody for the hapten in the coating antigen is important for improving assay sensitivity. The 2D-QSAR model of the OPs suggested that increasing the E_{LUMO} of a compound might decrease

(41) Wie, S. I.; Hammock, B. D. *J. Agric. Food Chem.* **1984**, *32*, 1294–1301.

(42) Galve, R.; Sanchez-Baeza, F.; Camps, F.; Marco, M. P. *Anal. Chim. Acta* **2002**, *452*, 191–206.

(43) Greirson, B. N.; Allen, D. G.; Gare, N. F.; Waston, I. M. *J. Agric. Food Chem.* **1991**, *39*, 2327–2331.

(44) Goodrow, M. H.; Hammock, B. D. *Anal. Chim. Acta* **1998**, *376*, 83–91.

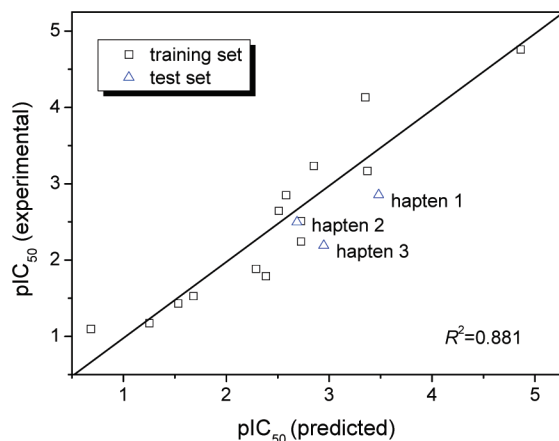


Figure 5. Plot of predicted versus experimental values (pIC_{50}) by using the topomer CoMFA.

antibody recognition. From the graphical representation of the OPs LUMO (Figure 3), it is obvious that changing the structure of the phenyl substituent might change the antibody recognition for the analytes. To increase the E_{LUMO} of a compound, the phenyl substituent was replaced by a linear alkane chain, which resulted in the design of hapten 2 (Figure 1). The E_{LUMO} of hapten 2 was estimated to be 0.004 52 au, which was higher than that of hapten 1 (−0.046 54 au). From the 3D-QSAR model, an alkane substituent located at the meta-position of phenol might decrease antibody recognition, resulting in the design of hapten 3 (Figure 1).

To validate the predictability of the obtained QSAR model, hapten 2 and hapten 3 were synthesized by a simple one step reaction and tested in the developed ciELISA. Plots of predicted versus experimental activity are presented in Figures 2 and 5. As revealed, both of the two QSAR models showed good predictability; the antibody showed lower affinity to the newly designed haptens than it did to hapten 1.

Development of a Heterologous ciELISA. Hapten 2 and hapten 3 were coupled to OVA for use as coating antigens to develop two heterologous ciELISAs, and the results are shown in Table 1. It is obvious that the assay sensitivity was significantly improved by using the heterologous ciELISA format. It also was found that using hapten 2–OVA as the coating antigen could better improve the assay sensitivity than by using hapten 3–OVA, even though the antibody affinity for hapten 3 was less than for hapten 2. The reason for this is hypothesized to be due to the presence of a similar spacer arm on hapten 3 as is used on hapten 1. The affinity of the antibody to the spacer arm was not eliminated. Hapten 2 consisted only of the *O,O*-diethyl thiophosphate moiety with no phenyl substituent. Compared with hapten 1, the heterology of hapten 2 was greater than that of hapten 3. Therefore, decreasing the affinity and increasing the heterology of the coating hapten were both important for the design of a new competitor to improve assay sensitivity. Using only a partial structure of the target molecule (or immunizing hapten) as the coating hapten may be a good strategy.

The ciELISA using hapten 2–OVA as the coating antigen showed high CR and sensitivity to eight *O,O*-diethyl OPs (Table 1). The LODs for parathion, coumaphos, dichlofenthion, phoxim, quinalphos, and triazophos were lower than 0.012 $\mu\text{g}/\text{mL}$, and they were lower than 0.055 $\mu\text{g}/\text{mL}$ for phosalone and phorate.

The broad-specificity immunoassay method presented here potentially can be used as a screening method for the simultaneous determination of *O,O*-diethyl OPs in environmental and food samples. The further application of the developed immunoassay in actual samples is currently being carried out.

CONCLUSIONS

In this study, a mAb against a generic hapten was raised and used to develop a homologous broad-specificity immunoassay for 14 *O,O*-diethyl OPs. A Gaussian calculation was applied to optimize the OP minimum energy conformations, and then structural parameters (including the hydrophobic, electronic, quantum-chemical, as well as geometrical parameters) were obtained. A multiple linear regression analysis was then used to obtain a 2D-QSAR model describing the antibody activity and the OP structural parameters. The results indicated that the lowest unoccupied molecular orbital (E_{LUMO}) and log of the octanol/water partition coefficient ($\log P$) of the OP compounds were mainly responsible for antibody recognition. Decreasing the E_{LUMO} or $\log P$ of an OP compound used as the coating hapten might improve antibody recognition. A 3D-QSAR model using topomer CoMFA was further obtained to study antibody recognition at the 3D level. It is convenient and useful to determine the steric and electrostatic interactions of compounds that affect antibody recognition through the use of a 3D-QSAR model resulting in contour maps.

On the basis of the above QSAR studies, two heterologous coating haptens (hapten 2 and hapten 3) were designed and applied to test the predictability of the obtained model. The consistency of the predicted and experimental data indicated good predictability of the model. On the basis of the two newly designed coating haptens, heterologous ciELISAs were developed. The use of a coating antigen with greater heterology (hapten 2) can better improve assay sensitivity compared to using hapten 3, even though the antibody affinity to hapten 3 was lower than that of hapten 2. The developed heterologous ciELISA showed high cross-reactivity and good sensitivity for eight *O,O*-diethyl OPs.

The results of this study suggest that molecular modeling is important for studying the interactions between an antibody and analytes. The molecular modeling results were useful for improving the immunoassay features by redesigning the coating hapten. Molecular modeling is also useful to direct the redesign of the immunizing hapten to obtain antibodies with broader-specificity and higher-sensitivity. Further studies with that aim are currently in progress at our laboratory.

ACKNOWLEDGMENT

This work was financially supported by the National High Technology Research and Development Program of China (Grants 2006AA10Z447 and 2007AA10Z437), the National Natural Science Foundation of China (Grant 30901005), and the Science and Technology Planning Project of Guangdong Province (Grant 2009A020101004).

Received for review July 10, 2010. Accepted September 14, 2010.

AC1018414